doi:10.1017/S1431927616004815
Microsc. Microanal. 22 (Suppl 3), 2016

Initial stages of Reduction of α-Fe_2O_3 Nanoblades

Wenhui Zhu[1], Jonathan P Winterstein[2], Renu Sharma[2] and Guangwen Zhou[1]

[1.] Department of Mechanical Engineering & Materials Science and Engineering Program, State University of New York, Binghamton, NY, USA
[2.] Center for Nanoscale Science and Technology, National Institute of Standards and Technology, Gaithersburg, MD, USA

The reduction of metal oxides is of great importance in a large variety of chemical and materials applications ranging from heterogeneous catalysis to electronic device fabrication. However, the fundamental knowledge of the atomic processes underlying the oxide reduction is still very limited. Several reasons contribute to the lack of this fundamental information including the difficulty of measurements of the atomistic processes of the reaction and the longstanding challenge in identifying the reaction mechanisms in heterogeneous systems. By manipulating the surface roughness of a Fe substrate, we recently demonstrated that various morphologies of iron oxide nanostructures, such as nanowires, nanbelts and nanoblades, can be obtained by thermal oxidation of Fe [1, 2]. We previously showed that the reduction of α-Fe_2O_3 nanowires proceeds via the ordering of oxygen vacancies followed by the transformation pathway of α-Fe_2O_3 → γ-Fe_2O_3 → Fe_3O_4 [3]. Here we extend the study to the reduction of α-Fe_2O_3 nanoblades using an environmental transmission electron microscope (ETEM).

The α-Fe_2O_3 nanoblades samples were prepared by thermal oxidation of sandblasted iron foils. As-prepared α-Fe_2O_3 nanoblades were transferred onto a Si_3N_4 membrane TEM window and then loaded into the ETEM. Pure dry hydrogen (99.999 %) was flowed into the ETEM column to achieve a partial pressure of 0.5 Pa. The sample was then heated up to 500 °C. The *in situ* observations of the oxide reduction were conducted under these conditions by time-resolved (video rate), high-resolution transmission electron microscopy (HRTEM) imaging, nano-diffraction and electron energy loss spectroscopy (EELS).

The TEM image in Fig 1a shows the typical morphology of the as-prepared α-Fe_2O_3 nanoblades. Fig. 1b is a nanodiffraction pattern obtained from the area marked with the red rectangle in Fig. 1a, which shows that the nanoblade has a bicrystal structure with a coincident-site-lattice (CSL) twist boundary (Σ boundary). The CLS twist boundary structure of two stacked crystals can be determined from the nano-diffraction pattern shown in Fig. 1b. The rotation angle of 21.8 ± 1° between the two α-Fe_2O_3 crystals along the <0001> directions matches with the Σ = 7 boundary structure (theoretical angle: 21.79°), and this CLS boundary structure is dominantly present among all the nanoblades examined. Fig. 1c is a crystal model based on the diffraction pattern in Fig. 1b and used for HRTEM image simulations. The HRTEM image shown in Fig. 1d matches well with the simulated image, with thickness of 4 nm and defocus of -9 nm, as marked by the red rectangle in Fig. 1d. The CLS twist boundary is not directly visible in the HRTEM image (Fig. 1d) because it is perpendicular to the electron beam.

Fig. 2a shows an HRTEM image of the nanoblade after 30 min of H_2 reduction at 500 °C and Fig. 2b is the nano-diffraction pattern of the same area shown in Fig. 2a. Indexing of the diffraction pattern shows that the parent α-Fe_2O_3 is partially transformed to γ-Fe_2O_3, with the rotation angle of 30° between the oxide phases and the <0001> of α-Fe_2O_3 (hexagonal structure) is parallel to the <111> of γ-Fe_2O_3 (cubic). Both the {0001} and {111} planes are the close-packed planes for the two Fe oxide phases,

evolved to the nearest stable arrangement of the two structures with a 30° rotation from the original value of 21.79°.

Fig. 3a shows the HRTEM of the same nanoblade with two regions with Moiré fringes where the two regions overlap. Fig. 3(b and c) are the diffractograms from areas marked by red square b and c in Fig. 3a. The extra spots in the diffractogram (b) indicate the formation of an intermediate structure with superlattice due to the ordering of oxygen vacancies parallel to {422} planes, i.e. d spacing = $3d_{\{422\}}$. Based on the white line ratios of Fe-L_3/L_2 edges in the EELS (Fig. 3(d and e)), we can infer that the two structures are γ-Fe_2O_3 and Fe_3O_4, respectively. The continuous supply of H_2 provided a driving force for the metastable γ-Fe_2O_3 to transform into stable Fe_3O_4 via the formation of a γ-Fe_2O_3 superlattice due to oxygen-vacancy ordering [4].

References:
[1] Yuan, L., et al., Nanoscale, 2013. **5**(16): p. 7581-7588.
[2] Yuan, L., et al., Materials Science and Engineering: B, 2012. **177**(3): p. 327-336.
[3] Zhu, W., et al., Microscopy and Microanalysis, 2015. **21**(SupplementS3): p. 995-996.
[4] Chen, Z.Q., et al., Chemistry of Materials, 2008. **20**(9): p. 3224-3228.

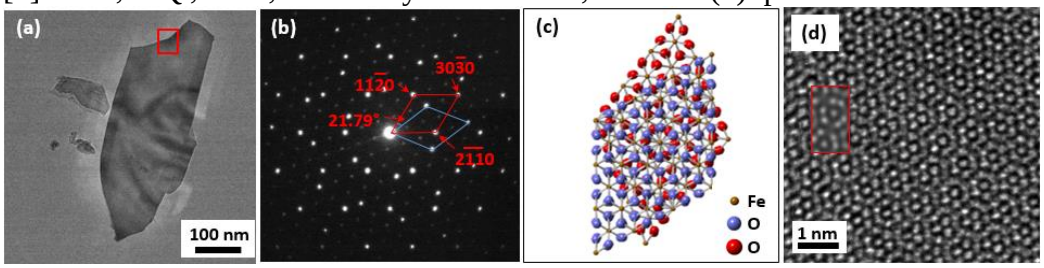

Figure 1. (a) TEM image of a typical piece of nanoblade. (b) Nanodiffraction pattern of the marked area in (a), showing it is a coincidence-site-lattice with a 21.79° rotation. (c) Crystal structural model built based on the diffraction analysis in (b). (d) HRTEM image of the nanoblade, with the inset of matched simulated one using the model in (c).

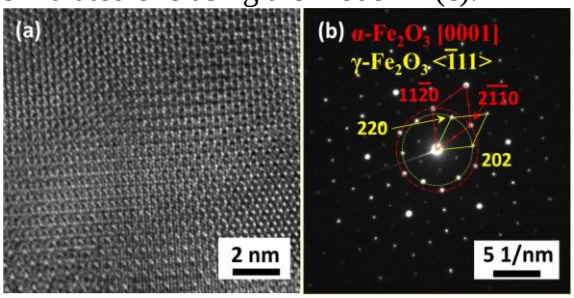

Figure 2. The HRTEM (a) and nanodiffraction pattern (b) of the nanoblade showing a transition phase during the reduction. The coincidence-site-lattice transformed into a layered structure of α-Fe_2O_3 and γ-Fe_2O_3, with a 30° rotation.

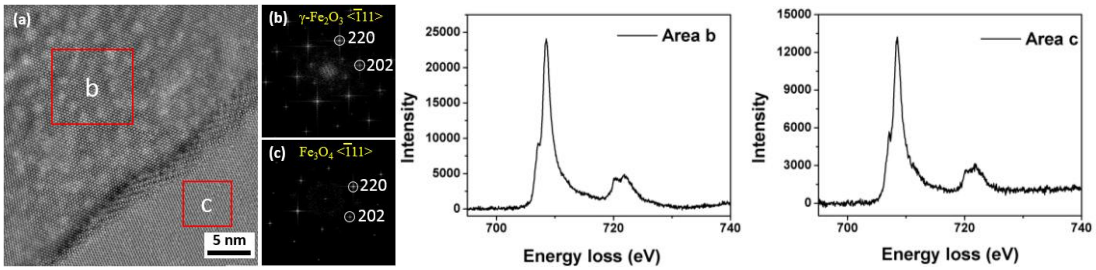

Figure 3. (a) HRTEM image showing the transformation from γ-Fe_2O_3 superlattice to Fe_3O_4. (b and c): the diffractograms from area b and c, respectively. Note the extra spots in (b). (d and e): EELS spectra of Fe L edge from area b and c. Their phases were determined by the white line ratios of Fe L.

https://doi.org/10.1017/S1431927616004815 Published online by Cambridge University Press